Available online at www.sciencedirect.com
SCIENCE DIRECT®
European Journal of Medicinal Chemistry 38 (2003) 587–595
EUROPEAN JOURNAL OF MEDICINAL CHEMISTRY
www.elsevier.com/locate/ejmech

Original article

The enhancement of neutron irradiation of HeLa-S cervix carcinoma cells by cell–nucleus-addressed deca-*p*-boronophenylalanine

Klaus Braun [a,*], Gerd Wolber [b], Waldemar Waldeck [c], Rüdiger Pipkorn [d], Jürgen Jenne [a], Ralf Rastert [a], Volker Ehemann [f], Andreas Eisenmenger [b], Heike Corban-Wilhelm [a], Isabell Braun [g], Stefan Heckl [e], Jürgen Debus [a]

[a] *Clinical Cooperation Unit Radiation Oncology, German Cancer Research Center, Im Neuenheimer Feld 280, 69120 Heidelberg, Germany*
[b] *Division of Biophysics and Medical Radiation Physics, German Cancer Research Center, Heidelberg, Germany*
[c] *Division of Biophysics of Macromolecules, German Cancer Research Center, Heidelberg, Germany*
[d] *Central Section for Peptide Synthesis, German Cancer Research Center, Heidelberg, Germany*
[e] *Division of Radiological Diagnostics and Therapy, German Cancer Research Center, Heidelberg, Germany*
[f] *Institute of Pathology, University of Heidelberg, Heidelberg, Germany*
[g] *Department of Radiation Therapy, University of Marburg, Marburg, Germany*

Received 10 January 2003; received in revised form 31 March 2003; accepted 3 April 2003

This article is dedicated to Harald zur Hausen on the occasion of his retirement as Head of the German Cancer Research Center with gratitude and appreciation for 20 years of leadership

Abstract

Boron neutron capture therapy (BNCT) is an experimental treatment modality which depends on a sufficient cellular uptake of Boron (^{10}B) followed by an exposure to a thermal neutron beam from a nuclear reactor. High energetic particles (^{4}He and ^{7}Li) are created during the neutron capture reaction and produce DNA damages, which lead to cell killing. Regarding BNCT, the short radiation range of He- and Li-particles is decisive for the distribution of ^{10}B. Until now, BNCT has been lacking for therapeutically effective concentrations of ^{10}B. Twenty-four hours after the combined use of our 'Bioshuttle'-*p*-borono-phenylalanine$_{10}$-constructs ('Bioshuttle'-*p*-BPA$_{10}$) and neutron-irradiation, an obvious reduction of the radiation-resistant HeLa-S cells could be observed. No cells were alive 72 h after the incubation with 'Bioshuttle'-*p*-BPA$_{10}$ followed by neutron irradiation. A post-mitotic cell death could be assumed based on flow cytometrical data.

Keywords: Bioshuttle; Boron neutron capture therapy (BNCT); Boronophenylalanine (BPA); Drug delivery; LET-effects; Nuclear transport

1. Introduction

Cervix carcinomas represent the second most frequent female tumor worldwide. More than 471,000 new cases are diagnosed each year.

Irradiation is the most commonly used adjuvant therapy of cervix carcinomas. Unfortunately, in some cases sublethal irradiation dosages result in a significant growth advantage of radiation-resistant tumor cells [1]. Therefore, a possible recurrence of cervix carcinoma after irradiation could deteriorate the patient's prognosis [2]. In this situation, the boron neutron capture therapy (BNCT) could produce relief.

Biological and therapeutic effects of neutrons were first described in 1936 [3]. The presently used NCT concept seems to be a reliable method. However, only a slight effect is observed after using neutrons alone. Thermal neutrons alone (<0.4 eV) release energy in insufficient levels with respect to cell killing. The capture of thermal neutrons by ^{10}B results in a high energy linear transfer (LET) radiation by the ^{10}B(n/α)^{7}Li reaction [4]:

$$^{10}\mathrm{B} + ^{1}n \rightarrow [^{11}\mathrm{B}]^{*} \rightarrow ^{7}\mathrm{Li} + ^{4}\mathrm{He} + \gamma + 2.79\ \mathrm{MeV}$$

* Corresponding author.
E-mail address: k.braun@dkfz.de (K. Braun).

0223-5234/03/$ - see front matter
doi:10.1016/S0223-5234(03)00088-6

Using the BNCT strategy, irradiation of different tumors seems possible. Tumor cells are first exposed to a stable non-radioactive ^{10}B isotope and further to thermal neutrons captured by the ^{10}B. This capture results in a splitting of the excitated $^{11}B^*$ nucleus releasing both a high energy α-particle and ^{7}Li (range about 9–14 μm), which in turn leads to cell-destruction. The surrounding healthy tissue remains undamaged [5–8]. A successful BNCT requires a boron concentration to 20–35 μg g^{-1} tumor or 10^9 ^{10}B atoms per cell [9,10].

The central pharmacological question referring to the efficient ^{10}B delivery could not be solved simply by using higher ^{10}B application dosages. During brain tumor irradiation, high ^{10}B concentrations in blood and brain tissue would lead to extensive toxic damage of both the tumor and the healthy surrounding tissue. Furthermore, until now a successful treatment has been prevented by an insufficient nucleus-directed delivery of ^{10}B.

There have been several studies in which the authors tried to optimize the delivery of ^{10}B. Up to now, BPA (boronophenylalanine) and BSH (borane-sulfhydryl-; $Na_2B_{12}H_{11}SH$) found use in clinical BNCT trials. An accumulation of BSH in SCCVII tumor cells could not be observed [11]. The accumulation of ^{10}B (BSH) in tumor cells after using electroporation was controversly discussed [12]. A recent report describes the synthesis and use of new azanonaboranes contains eight boron atoms [13]. Despite several efforts dealing with the problem of insufficient nuclear ^{10}B uptake, a suitable solution has not yet been found. However, a possible therapeutical effect of BNCT could be optimised by a sufficient nuclear ^{10}B accumulation. We tried to reach high intracellular ^{10}B concentrations by modifying the ^{10}B components and ameliorating the cell nucleus-directed ^{10}B transport. Therefore, in case of chemo- and radiation-therapy resistant tumors, BNCT could be the future treatment of choice. For this reason, our major aim was to optimize the delivery of BPA and to reach a high nuclear ^{10}B accumulation. To circumvent obstacles concerning delivery of ^{10}B we have developed a highly efficient cell nucleus-addressed non-viral delivery system ('Bioshuttle') [14] by which a high nuclear ^{10}B concentration could be achieved. This non-viral delivery system consists of a 10-mer L-*p*-boronophenylalanine$_{10}$ (*p*-BPA$_{10}$) which is covalently bound to a nuclear localization sequence (NLS) resulting in the product called 'Bioshuttle-NLS-L-*p*-boronophenylalanine$_{10}$' ('Bioshuttle'-*p*-BPA$_{10}$). The 'Bioshuttle'-*p*-BPA$_{10}$ represents a drug delivery system to cross the cellular membranes of HeLa-S cervix carcinoma cells. Internalisation and localization of the 'Bioshuttle-*p*-BPA$_{10}$' could be confirmed with laser desorption mass spectrometry and confocal laser scanning microscopy (CLSM), respectively.

2. Chemistry

2.1. Chemical synthesis and purification of L-*p*-boronophenylalanine$_{10}$

2.1.1. Chemical synthesis of deca-*p*-boronophenylalanine

The Fmoc protected L-BPA was carried out according to standard procedures [15].

The L-*p*-boronophenylalanine monomer was obtained from Ryscor Science Inc. 3209 Gresham Lake Rd. RALEIGH, NC 27615, USA (Cat. No.: 5002). To perform solid phase synthesis we used the Fmoc-strategy in a fully automated multiple synthesizer Syro II (MultiSyn Tech, Germany). The synthesis was carried out on 0.05 mmol Tenta Gel R RAM 0.18 mmol g^{-1} of substitution (Rapp-Polymere GmbH D-72072 Tübingen). The C-terminal Fmoc BPA residue was attached to the Rink-Linker, which ensured a peptide amide after final acid treatment. *O*-(Benzotriazol-1-yl)-*N*,*N*,*N*′,*N*′-tetramethyluroniumhexa-fluorophosphate (HBTU) served as a coupling agent. The protected peptidyl resin was first treated with 20% piperidin in dimethylformamide for 12 min and further washed thoroughly with dimethylformamide. Cleavage and deprotection of the peptide resin were achieved by treatment with 90% trifluoroacetic acid, 5% ethanedithiol, 2.5% thioanisol, 2.5% phenol (v/v/v) for 2.5 h at room temperature. Sequences of single modules as well as the complete modular construct are characterized with analytical HPLC (Shimadzu LC-10) and laser desorption mass spectrometry (Finnigan, Vision 2000) as follows [16]. The random NLS constructs were synthesized in identical procedures. The Alexa®Fluor546-labelled transport peptide, and the FITC-labelled L-*p*-boronophenylalanine$_{10}$ peptides were synthesized in identical procedures.

2.1.2. Peptide purification

All products were precipitated in ether and purified by preparative HPLC (Shimazu LC-8A, Japan) on a YMC ODS-A 7A S-7 μm reverse phase column (20 × 250 mm) using of 0.1% trifluoroacetic acid in water (A) and 60% acetonitrile in water (B) as eluent. Peptides were eluted with a successive linear gradient increasing from 25 to 60% B-eluent in 49 min at a flow rate of 10 mL min^{-1}. The fractions corresponding to the purified conjugate were lyophilized. Sequences of single modules as well as the complete modular construct are characterized with analytical HPLC (Shimadzu LC-10, Japan) using a YMC-Pack Pro C18 (150 × 4.6 mm ID) S-5μm, 120A-column with 0.1% trifluoroacetic acid in water (A) and 20% acetonitrile in water (B) as eluent. The analytical gradient ranged from 5 (B) to 80% (B) in 35 min. Further characterization was performed with laser desorption mass spectrometry (Finnigan, Vision 2000). Cysteine groups of the transmembrane peptides TPU

TQVKIWFQNRRMKQKKC (see Table 3) and the NLS peptide module ^{10}B-compound {(^{10}BPA)$_{10}$-KK-PKKKRKVC (NLS$_{SV40T}$)} (see Table 3) were oxidized at the range of 2 mg mL^{-1} in a 20% DMSO water solution. Five hours later the reaction was completed. The random sequence peptide (see Table 3) was linked under identical conditions. The progress of oxidation was monitored by analytical C18 reverse phase HPLC.

3. Pharmacology

3.1. Cell culture

The experiments were performed with the HeLa-S cervix carcinoma cells (DKFZ tumorbank), cultured in Joklik Minimal Essential Medium medium (MEM-Joklik) (Sigma Aldrich #8028), supplemented with 10% fetal bovine serum (FBS, Sigma, Germany) and 2 mM glutamine (Sigma, Germany) at 37 °C in 5% CO_2 atmosphere. Cells were grown in a mycoplasma free status as monitored by PCR (Mycoplasma PCR Primer Set, Stratagene, Germany).

3.2. Boron uptake efficiency by mass spectrometry

The uptake of 'Bioshuttle'-*p*-BPA$_{10}$ was examined by a mass spectrometrical method.

^{10}B concentration measurements were carried out by means of a high resolution element mass spectrometer (Finnigan MAT ELEMENT2, Bremen, Germany) with inductively coupled plasma (ICP-MS) at a resolution ($\Delta m \times m^{-1}$) of 4000. The instrument was equipped with a self aspirating 100 μL min^{-1} PFA-Nebulizer and spray chamber, standard injector and torch. Instrument and operation parameters were as follows: plasma power = 1100 W, cool gas flow = 15.5 L min^{-1}, auxiliary gas flow = 1 L min^{-1}, sample gas flow = 1 L min^{-1}, mass window = 850%, search window = 800%, integration window = 80%, samples per peak = 30, No. of scans = 3[10]. Internal standard correction and drift correction was active for ^{103}Rh (for ICP, Merck, Germany, diluted to 5 ng mL^{-1}). Also ^{11}B was measured to monitor a possible contamination of ^{10}B by ^{11}B. Before measurement the instrument was tuned and calibrated using 1 ng mL^{-1} multi-element standard solution (Merck, Germany).

3.2.1. Sample preparation

All preparations of samples and standards were carried out at clean flow box benches. For dilutions purified and background measured water was used (> 17.5 MΩ cm^{-1}).

A closed, pressurized microwave digestion unit (Mars5, CEM GmbH, Germany) equipped with a rotor for 14 vessels, each containing three Teflon® vessels with a volume of 3 mL was used for digestion of samples containing cellular components. Aliquots of 200 μL sample (cell nuclei) and 200 μL HNO_3 60% (grade: Ultra pur®, Merck, Germany) were digested as follows: Ramp of 15 min, 300 W, 100%, 0.5 bar, 150 °C, holding for 10 min, ramp of 15 min, 300 W, 100%, 0 bar to cool to room temperature, holding for another 5 min. The samples were diluted by additional 600 μL HNO_3. Before measurement 200 μL of the samples were diluted by 700 μL H_2O and 100 μL $^{103}RhCl_3$ standard solution (E. Merck, Darmstadt, Germany) was added. Two-hundred microlitres of cell free suspensions were diluted with 600 μL H_2O and 100 μL of HNO_3 and 100 μL of ^{103}Rh standard solution were added. According to the pretreatment, those 12 samples (cell nuclei) were each measured separately. Afterwards a standard curve was created from several differing ^{10}B concentrations. This standard curve as well as a second control curve (only clear water with no chemical ingredients) served for a comparable evaluation (ICP-MS).

3.3. Neutron source

Fast neutrons were produced by bombarding a thick beryllium target with 10–20 μA of protons (17, 25, 32 MeV) and deuterons (9, 11.5, 16 MeV) from the DKFZ negative ion cyclotron [17]. The neutron beams can be collimated by exchangeable ducts with field sizes of 13 × 13, 10 × 10, 8 × 8, 6 × 6, 3 × 3 cm^2 and a circular field of 1.8 cm diameter. Total fast neutron plus photon doses were measured using tissue equivalent ionization chambers (0.9 cm^3, PTW, $\alpha_c = 1.115 \times 10^7$ Gy C^{-1}; and 2.4 cm^3, Exradin, $\alpha_c = 2.98 \times 10^7$ Gy C^{-1}) made from A-150 plastic flushed gently with methane based tissue-equivalent (TE) gas. The output charge was corrected for ambient temperature and air pressure. The dosimetry system (UNIDOS, PTW; $U = +400$ V) was checked from time to time against a calibrated current source (Keithley 261 Picoampere Source). Differences remained below 10^{-3}.

The thermal neutron flux ϕ_{th} was determined by the gold/cadmium activation method, i.e. calculated from the difference of the saturation activities per cm^2 A_+, A_- of 8 mm ∅ ^{198}Au foils 50 μm thick with and without 1 mm Cd shielding, respectively, according to the activation equation [18]

$$A_\pm = Nd\sigma\phi_\pm \,\mathrm{SAC} \quad \text{or:} \quad \phi_\pm = A_\pm/Nd\sigma\,\mathrm{SAC} = C_\pm \tag{1a}$$

$$\phi_{th} = \phi_- - \phi_+, \text{ with } \phi_\pm = (R_\pm/m_\pm)[\exp(\lambda t_{a\pm})/(1-\exp(-\lambda t_{b\pm}))] \times 5.61 \text{ cm}^{-2}\text{ s}^{-1} \tag{1b}$$

here,

R_+, R_- = count rates (s^{-1}) of the detector from the gold foil with and without Cd cover, respectively. And, with the same meaning of the indices +, −, $m_\pm$ = masses (mg) of the gold foils (ca. 40 mg). $t_{a\pm}$ and $t_{b\pm}$ (h) = time of activation and time elapsed since the end of irradiation, respectively.

The last factor contains the effective absorption cross section of ^{197}Au for thermal neutrons $\sigma_{th,eff} = (1/2) \times \pi^{1/2}\sigma_0$ with $\sigma_0 = 98.8(5) \times 10^{-24}$ cm^2, the thickness d (μm) of the foils, the density N (cm^{-3}) of Au atoms in the foil, the photon decay probability of the 412 keV state of ^{198}Au (95.53%), the sensitivity ε of the Ge(Li) spectrometer used ($\varepsilon \cong 1\%$ at 50 mm distance from foil to crystal), the self absorption correction (SAC) { = 0.9 for 50 μm thick ^{197}Au foils [19]} as well as scaling factors.

The 412 kV photons of ^{198}Au ($T_{1/2} = 2695$, $d = 64.7$ h) were counted several times with 1–3 days delay to get some idea of the reproducibility of the method.

The procedure and calculations were checked by activating identically shaped gold foils in the central irradiation position ZBR of the Heidelberg TRIGA Research Reactor at reduced power (100 W). The results differed by +6% from the nominal value of ϕ_{th} in this ZBR position. From this, together with the uncertainties of the many physical parameters involved in Eqs. (1a) and (1b) we estimate the overall uncertainty of our results to be 10–15%.

Both, the naked and Cd covered gold samples were fixed on thin perspex slabs in a distance of about 2 cm. These twin probes and the ionization chambers were inserted into water filled bores 22 mm ∅ along a diameter of the circular perspex phantom 20 cm ∅, 13 cm high with different spacing of the bores. Their distance, i.e. the spatial resolution of the measurements in the phantom can be varied from 1.2 to 4 cm.

For the biological pilot experiment, the vials containing the HeLa-S cells with and without ^{10}B treated load were positioned in the same phantom in two bores close to the axis and irradiated with 32 MeV p-Be neutrons (1.5 Gy, large (13×13 cm^2) field size and 1 Gy, small (3×3 cm^2) field size). 1.5 Gy of 14 MeV neutrons result in ca. 20% survival [20]. The phantom was rotated by 360° to mimic rotation treatment. In this setting, the thermal neutron fluences amount to 3.6×10^{10} cm^{-2} (large field) and 0.62×10^{10} cm^{-2}. These values have an estimated uncertainty of 15%.

The BNCT dose in a ^{10}B-loaded volume can be estimated using a simple equation given by Sweet (1997):

$$D_{BNC} = F_{th} \times N \times \sigma_a \times E \times f \quad (2)$$

with

F_{th} = thermal fluence (cm^{-2}), derived from the measured flux Φ_{th} (cm^{-2} s^{-1})
N = number of ^{10}B atoms per unit volume (cm^{-3})
σ_a = capture cross section of ^{10}B for thermal neutrons (3385×10^{-24} cm^2)
E = Energy (MeV) imparted to the fission products ^{4}He and ^{7}Li (2.34 MeV on average = 3.7×10^{-13} J)
f = fraction of the energy absorbed in tissue.

Both fragments from ^{10}B have very short ranges of about 9–5 μm, their total energy released is deposited in the volume of approximately one cell. Hence, f can be taken as 1 if we disregard the small loss of radiation energy by the escape of the 0.48 MeV photons.

For a uniform concentration of 30 μg ^{10}B/g tissue (1.8×10^{18} ^{10}B atoms/g) Eq. (2) transforms into

$$D_{BNC} = F_{th} \times 2.6 \times 10^{-2} \text{ cm}^2 \text{ J kg}^{-1} = F_{th} \times 2.6 \text{ cGy} \quad (3)$$

with F_{th} in units of 10^{10} cm^{-2} and tissue density set = 1 g cm^{-3} [21].

3.4. Flow cytometry

Flow cytometrical analysis were performed using a PAS II flow cytometer (Partec, Münster/Germany) equipped with mercury vapour lamp 100 W and filter combination for 2,4-diamidino-2-phenylindole (DAPI) stained single cells. From natively collected probes the cells were isolated with 2.1% citric acid/0.5% Tween 20™ with modifications at room temperature by slightly shaking [22]. Phosphate buffer (7.2 g $Na_2HPO_4 \times 2H_2O$ in 100 mL H_2O dest.) pH 8.0 containing DAPI for staining the cell suspension was prepared. 3×10^4–1×10^4 cells are represented in one histogram to measuring DNA-index and cell cycle. To perform histogram analysis the Multicycle program (Phoenix Flow Systems, San Diego, CA) was used.

Human lymphocyte nuclei from healthy donors served as internal standard to determinate the diploid cell population. The mean coefficient of variation (CV) of the diploid lymphocytes was 0.8–1.0.

3.4.1. Cell viability

10^5 HeLa-S cells were incubated with the 'Bioshuttle'-p-BPA_{10} (100 pM) for 1 h and washed twice with MEM. The measurements were carried out after incubation times of 24, 48 and 72 h. Non-treated cells served as controls for the same time intervals.

The analysis was performed in a FACS Calibur flow cytometer (Becton Dickinson Cytometry Systems, San Jose, CA) using the forward- and side scatters and the relative fluorescence intensity of propidium iodide stained native cells on FL2-channel in a logarithmic scale (Cell Quest, Becton Dickinson). Dead cells were stained with propidium iodide, whereas in living cells the nuclei remain unstained. In a logarithmic histogram,

there are only little amounts of living cells remaining unstained (10^0–10^2), in contrast to the higher amounts of dead cells (10^3–10^4) nuclear stained with propidium iodide (see Fig. 1).

3.5. Confocal laser scanning microscopy

The intracellular distribution of the ‘^{ALEXA}Bioshuttle’-*p*-BPA_{10}^{FITC} (bi-labelled with ALEXA® 546 Fluor and FITC) (see Table 3 B) in HeLa-S cells was determined by a Zeiss laser confocal microscope (LSM 510 UV). To excite the FITC, a filter with 488 nm was used. The resulting emission was in turn filtered by a 522 nm set. In case of ALEXA® 546 Fluor, excitation was achieved by a 543 nm filter with subsequent filtering of the emission by a 580 nm filter. The optical slice thickness was 700 nm.

3.5.1. Composition of the ‘^{ALEXA}Bioshuttle’-*p*-BPA_{10}^{FITC} for CLSM

The modular built ‘^{ALEXA}Bioshuttle’-*p*-BPA_{10}^{FITC} consists of a cellular membrane transport peptide unit (TPU) and of a 10-mer boronophenylalanine (BPA) which is covalently linked to a nuclear localization sequence (NLS[SV40-T]) (see Table 3 B). As a control, a random NLS sequence was used (see Table 3 B). A Cysteine mediated cleavable disulfide bond enables the connection between the TPU and NLS (see Table 3 B).

3.5.2. ‘^{ALEXA}Bioshuttle’-*p*-BPA_{10}^{FITC} incubation of HeLa-S cells for CLSM

To perform fluorescence microscopic studies, 5×10^5 HeLa-S cells were seeded over 25 h into quadriPERM® plus (Heraeus, Germany; Cat. No.: 76077310) containing a sterile glass coverslip. To perform CLSM cells were rinsed twice in fresh MEM medium for a period of 10 min. A freshly prepared ‘^{ALEXA}Bioshuttle’-*p*-BPA_{10}^{FITC} solution with culture medium was added in a final concentration of 100 pM and incubated at 37 °C, 5% CO_2 atmosphere for 30 min. The culture medium was removed to start microscopic studies later. The cells were washed twice and were finally embedded in Moviol®.

4. Results

4.1. Mass spectrometrical evaluation of ^{10}B uptake efficiency

4.1.1. ^{10}B uptake after treatment with the ‘Bioshuttle’-*p*-BPA_{10} in combination with neutron irradiation

The ‘Bioshuttle’-*p*-BPA_{10} was applied to the HeLa-S cells 1 h before neutron irradiation. After 1 h incubation time the HeLa-S cells were centrifuged. The cell pellets were washed with culture medium twice and subsequently neutron irradiated. At the irradiation time point the ^{10}B concentration was quantified to reach a value of

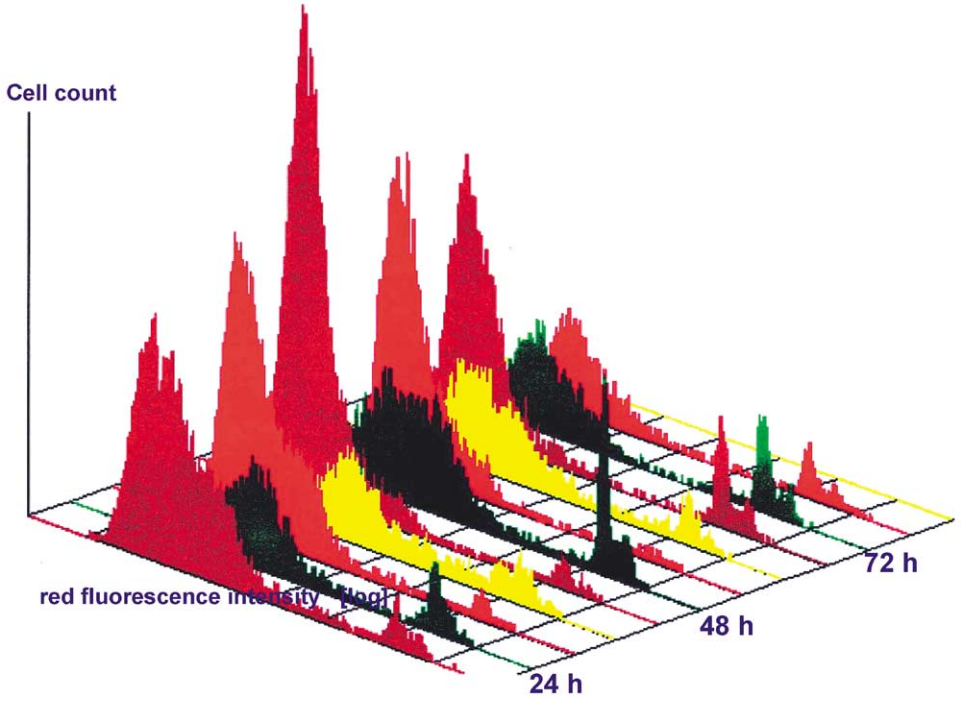

Fig. 1. Flow cytometry—cell-viability: Biological effect of neutron-irradiation with or without ‘Bioshuttle’-*p*-BPA_{10} in HeLa-S cells, after 24, 48 and 72 h. The cell viability was confirmed by using propidium iodide which only stains the nucleus in viable cells. ■, neutron irradiation and ‘Bioshuttle’-*p*-BPA_{10}; ■, neutron irradiation without ‘Bioshuttle’-*p*-BPA_{10}; ■, ‘Bioshuttle’-*p*-BPA_{10} without radiation; ■, untreated control cells

Table 1
Relative ^{10}B concentrations [ng g^{-1}] in the cell nuclei of HeLa-S cells (mass spectrometrical methods) 0, 24, 48 and 72 h after a single neutron irradiation dosage of 1.5 Gy

I Nucleus	II Nucleus	III Nucleus	IV Nucleus	(h)
170	7	175	4	0
115	4	220	5	24
135	3	225	4	48
–	3	215	4	72

I: Neutron irradiation and 'Bioshuttle'-*p*-BPA_{10}; II: neutron irradiation without 'Bioshuttle'-*p*-BPA_{10}; III: 'Bioshuttle'-*p*-BPA_{10} without irradiation; IV: untreated control cells.

170 ng g^{-1} in the cell nuclei (see Table 1). After 24 h the nuclear ^{10}B concentration decreased to 115 ng g^{-1} cell nuclei (see Table 1). Fourty-eight hours after irradiation ^{10}B concentrations of 135 ng g^{-1} were detected in the nuclei (see Table 1). Seventy-two hours after irradiation no cell nuclei could be measured.

4.1.2. *^{10}B uptake after sole treatment with the 'Bioshuttle'-p-BPA_{10}*

In previously non-irradiated control cells, after incubation the nuclear ^{10}B concentrations were 175, 220, 225 and 215 (ng g^{-1}) 0, 24, 48 and 72 h, respectively (see Table 1).

4.2. *Intracellular* '^{ALEXA}Bioshuttle'-*p*-BPA_{10}^{FITC} *localization by CLSM*

Dual staining of the '^{ALEXA}Bioshuttle'-*p*-BPA_{10}^{FITC} was performed to determine whether ALEXA® 546 Fluor and FITC fluorescent signals were localized in the cytoplasm or in the nucleus of HeLa-S cells. HeLa-S cells treated with '^{ALEXA}Bioshuttle'-*p*-BPA_{10}^{FITC} (see Table 3 B) showed different fluorescence signals in both the cytoplasm and the nucleus (see Fig. 2). A mixed fluorescence signal (ALEXA® 546 Fluor–red and FITC–green) was detected within the cytoplasm, whereas a sole green fluorescence signal (FITC) was observed in the cell nucleus (see Fig. 2). In case of linking the transport module and the *p*-BPA_{10}^{FITC} by a random NLS (see Table 3 B) there was only a cytoplasmic but no nuclear staining (see Fig. 3), which demonstrates the important function of the NLS for the nuclear delivery of *p*-BPA_{10}^{FITC}. The cytoplasmic cleavage of the two modules (TPU) and the resulting nuclear import of the FITC-tagged *p*-BPA_{10} lead to the nuclear *p*-BPA_{10}^{FITC} localization.

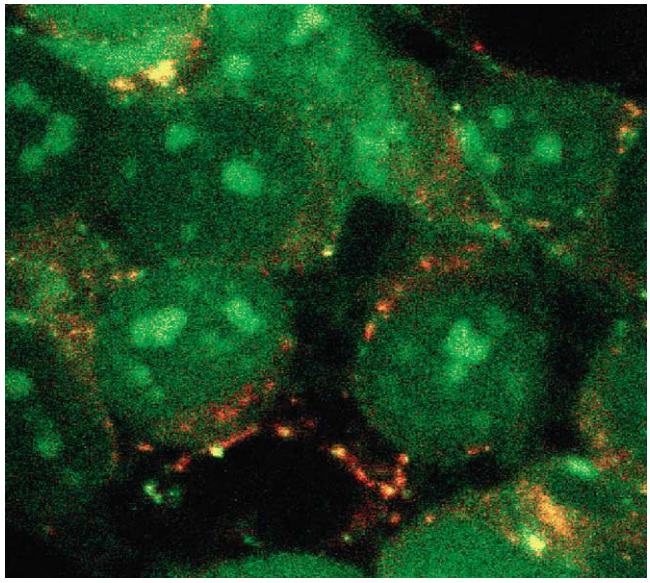

Fig. 2. Optical sections (CLSM) of living HeLa-S cervix carcinoma cells incubated with '^{ALEXA}Bioshuttle'-*p*-BPA_{10}^{FITC} harbouring a cleavable disulfide linker (Table 3b). The distribution of the '^{ALEXA}Bioshuttle'-*p*-BPA_{10}^{FITC} fluorescence in living HeLa-S cells shows a mixed red/green fluorescence signal (orange) in a punctuate staining pattern in the cytoplasm, whereas the cell nuclei were dominated by the green fluorescence signal. Cells were incubated with '^{ALEXA}Bioshuttle'-*p*-BPA_{10}^{FITC} for a period of only (final concentration 100 pM) 30 min.

4.3. *Flow cytometry*

Cell viability—Grouping of morphologically intact HeLa-S cells by their viability grade in viable, membrane damaged and dead cells.

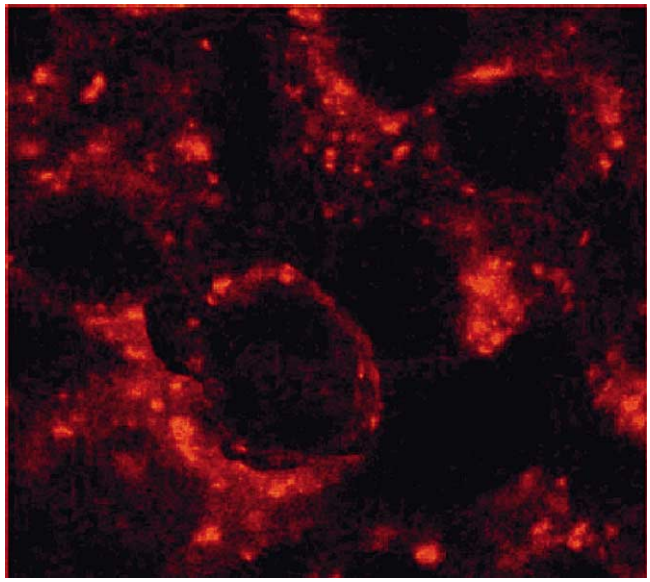

Fig. 3. Optical sections (CLSM) of living HeLa-S cervix carcinoma cells incubated with '^{ALEXA}Bioshuttle'-*p*-BPA_{10}^{FITC} harbouring a random NLS and a cleavable disulfide linker (Table 3b).

Table 2
Flow cytometry

		A	B		
		Whole fraction of intact cells	Subdivision of A		
			Viable	Membrane-damaged	Dead
24 h					
I	'Bioshuttle'-*p*-BPA_{10}+neutron irradiation	25.5	54.8	22.7	18.7
II	Neutron irradiation	54.2	92.1	3.9	3.5
III	'Bioshuttle'-*p*-BPA_{10} without irradiation	25.2	76.6	4.9	16.8
IV	Untreated control	54.9	90.0	3.5	5.9
48 h					
I	'Bioshuttle'-*p*-BPA_{10}+neutron irradiation	29.9	80.7	6.3	12.6
II	Neutron irradiation	48.7	93.4	2.9	3
III	'Bioshuttle'-*p*-BPA_{10} without irradiation	21.3	74.5	5	20.5
IV	Untreated control	67.3	94.6	1.8	3.4
72 h					
I	'Bioshuttle'-*p*-BPA_{10}+neutron irradiation	0	0	0	0
II	Neutron irradiation	20.8	79.2	4.6	16.
III	'Bioshuttle'-*p*-BPA_{10} without irradiation	26.8	72.4	5.2	22.3
IV	Untreated control	47.7	85.7	2.9	12.1

A: Percentage of morphologically intact cells after incubation with 'Bioshuttle'-*p*-BPA_{10} and neutron irradiation.B: Further subdivision of the whole fraction of intact cells in viable, membrane damaged and dead cells.

To prove the efficiency of both, our modified BNCT (neutron irradiation-effect combined with a 'Bioshuttle'-*p*-BPA_{10}) and the sole use of 'Bioshuttle'-*p*-BPA_{10}, flow cytometrical viability tests were performed. In both cases the final 'Bioshuttle'-*p*-BPA_{10} concentration was 100 pM, which is equivalent to ^{10}B concentration of 1 nM.

4.3.1. The influence of the 'Bioshuttle'-p-BPA$_{10}$ in combination with the neutron irradiation on the cell viability

Irradiation combined with 'Bioshuttle'-*p*-BPA_{10} leads after 24, 48 and 73 hours to percentages of surviving cells of 25.5, 29.9 and 0% with respect to the morphologically intact cells.

Regarding the first 24 h interval after incubation, most of the cells were alive (54.8%) whereas only 18.5% were dead and the remaining 22.7% were partially damaged in the membrane but seem intact (see Table 2). After 48 h the fraction of morphologically intact cells had further expanded (29.9%) with a decrease of the membrane damaged cells (6.3%) and dead cells (12.6%). In contrast, the number of viable cells obviously increased (80.7%). However, after 72 h this situation changed dramatically with no HeLa-S cells alive (see Table 2).

Table 3

A			
	Single module	Abbreviation	
1	transport peptide-unit	TPU (hum) Genebank AC P09629	TQVKIWFQNRRMKQKKC [b]
2	address peptide	NLS(SV40-T)	PKKKRKVC [b]
3	L-*p*-boronophenylalanine	*p*-BPA_{10}	$[C_9H_{12}BNO_4]$ [a]
Spacer variant			
a	neutron irradiation	-GG- [b]	
b	CLSM	-GK(FITC)	
B			
	Conjugate		
a	TPU-C [c]C-NLS-GG-[L-*p*-BPA]$_{10}$	neutron irradiation	
b	ALEXATPU-C [c]C-NLS-GK(FITC)-[L-*p*-BPA]$_{10}$	CLSM	
	ALEXATPU-C [c]C-Random-GK(FITC)-[L-*p*-BPA]$_{10}$	CLSM	

A: Chemical design of the transport modules used in the study.B: Chemical design of the 'Bioshuttle'-*p*-BPA_{10}.
[a] Rationalized formula.
[b] Single letter amino acid code.
[c] Cleavable disulfide spacer.

4.3.2. The sole effect of the 'Bioshuttle'-p-BPA$_{10}$ on the cell viability

The percentage of the morphologically intact cell group after incubation with the 'Bioshuttle'-*p*-BPA$_{10}$ was 76.7, 74.5 and 72.4% after 24, 48 and 72 h, respectively.

Twenty-four hours after incubation the percentage of viable cells within the morphologically intact cell fraction was 76.6% whereas 16.8% were dead. After 48 h this percentage of viable cells was 74.5% and 72.4% after 72 h (see Table 2). The percentage of membrane damaged cells remained nearly the same.

4.3.3. The sole effect of neutrons on the viability of HeLa-S cells

The percentage of the morphologically intact cell group after neutron irradiation was 92.1, 93.8 and 79.2% after 24, 48 and 72 h, respectively (see Table 2). We further examined three post-irradiation time points (24, 48 and 72 h) for membrane damaged cells out of the morphologically intact cell group. After 24, 48 and 72 h the amount of membrane damaged cells was 3.9, 2.9 and 4.6%, respectively (see Table 2).

5. Discussion and conclusion

The results demonstrate the different effects of neutron-irradiation, 'Bioshuttle'-*p*-BPA$_{10}$ treatment alone and combined treatment. The fraction of surviving cells (about 20%) after sole irradiation with fast neutrons (1.5 Gy of 14 MeV) was previously described [20] and could be confirmed by our results (20.9%) (see Table 2).

Flow cytometrical viability tests in HeLa-S cells after 24 h revealed, that after the sole treatment with the 'Bioshuttle'-*p*-BPA$_{10}$, 16.8% of all the examined cells were dead. That implicates a slight cytotoxic property of the ^{10}B delivered by the 'Bioshuttle' transporter (see Table 2). Based on the specific nuclear ^{10}B-delivery via our 'Bioshuttle'-*p*-BPA$_{10}$ a dose-reduction in future studies seems possible.

To realize a more efficient and economical therapy strategy of neutron-irradiation we have ameliorized the ^{10}B uptake- and targeting-system to obtain therapeutic relevant ^{10}B amounts by use of a transport and cell nucleus directed 'Bioshuttle'-*p*-BPA$_{10}$. Due to the use of small amounts of ^{10}B (1 nM = 100 pM × 10-mer PBA) it was previously not justified to expect any treatment effect. However, this revealed untrue by reaching survival-rates of about 20% after using our 'Bioshuttle'-*p*-BPA$_{10}$. This underlines the high efficiency of our conjugate, which might be explained by both the efficacy of the delivery system and the specificity for the cell nucleus.

To confirm the previous results, flow cytometry was used. The HeLa-S cells could be divided in morphologically intact and non-intact cell fractions. The fraction of these intact cells was further subdivided into three groups, namely viable, cells with slight membrane damages and dead ones (see Table 2). Dead cells can also be identified by staining with propidium iodide. This dye is excluded from live cells (with intact cell membranes) but is free to diffuse into dead cells and also in cells with smooth membrane disruptions which seem intact [24]. It should be mentioned that 24 h after the dual-treatment with neutron-irradiation and 'Bioshuttle'-*p*-BPA$_{10}$ incubation, the total amount of membrane damaged cells was 22.7%. After 48 h this percentage was further reduced to 6.3%. Astonishingly, there was a change in the amount of viable cells after 24 h (54.8%) compared to that after 48 h (80.7%), which could be explained by DNA repair mechanisms [23,7](see Table 2). Seventy-two hours post incubation time, the situation changed again with no cells alive (see Table 2). Flow cytometrical data indicate a post-mitotic cell death after initial irradiation and an incubation with 'Bioshuttle'-*p*-BPA$_{10}$ for a period of 72 h.

The high nuclear ^{10}B concentration can be explained by the active 'Bioshuttle'-*p*-BPA$_{10}$-mediated ^{10}B delivery into the cell nuclei of HeLa-S cells, which was mass spectrometrically confirmed (see Table 1). The decreased amounts of ^{10}B in the cell nuclei 24 h after neutron irradiation compared to that after incubation with the 'Bioshuttle'-*p*-BPA$_{10}$ alone (115 vs. 220 ng g^{-1}) could be explained by a radiation-induced reduction of the cellular metabolism with the exception of repair mechanisms [23]. The increase of the nuclear ^{10}B concentrations 48 h after incubation (see Table 1) could be explained by a subsequent reactivation of the nuclear transport systems still after the ending of cellular damage repair [23].

To validate the final result after the intracellular behaviour of the '^{ALEXA}Bioshuttle'-*p*-BPA$_{10}^{FITC}$, a double staining was achieved by using both, a red coloured fluorescence tag (Alexa® 546 Fluor) covalently bound to the TPU and a green fluorescence label (FITC) linked to the NLS–*p*-BPA$_{10}$ (see Table 3). The intracellular *p*-BPA$_{10}$ localization was confirmed by CLSM. Our results obviously show an enhanced active transfer of *p*-BPA$_{10}$ into the nucleus of living HeLa-S cells even at low concentrations (see Table 1). Two factors are identified as a prerequisite for nuclear translocation: (a) the efficient cytoplasmic delivery of the 'Bioshuttle'-*p*-BPA$_{10}$; and (b) an accessible and biologically active NLS sequence [14]. This has also been demonstrated in an earlier paper by molecular imaging using a Gd^{3+} construct [26].

Due to the need of high ^{10}B-concentrations in all previous studies, BNCT remained restricted to the experimental stage [4,5,11].

We could improve the ^{10}B-delivery by using a nuclear specific transport system.

The combination of the thermal neutron beam and the application of 'Bioshuttle'-*p*-BPA$_{10}$ could kill radiation-resistant HeLa-S cervix carcinoma cells. The effect on tumor cells by BNCT could overcome the tumor cell survival after the radiotherapy by photons [2].

Finally, with respect to the future treatment of cancer, two major conclusions could be drawn from our results.

First, in case of radiation-resistant HeLa-S cervix carcinoma cells, thermal neutron irradiation combined with 'Bioshuttle'-*p*-BPA$_{10}$ treatment could be more effectively compared to the conventional treatment with photon-irradiation. The specific delivery of ^{10}B into the cell nucleus is a decisive factor for a therapeutically useful BNCT [25]. Second, our in vitro results after the dual-treatment of thermal neutrons and our 'Bioshuttle'-*p*-BPA$_{10}$, could make a future application in vivo conceivable.

Our future aim is to develop NCT strategies for other tumors than the above mentioned.

Our modified BNCT technique should be expanded to other therapy-resistant tumors like those in the brain, breast, kidney, lung, pancreas and prostate.

References

[1] H. Utsumi, M. Ichihashi, T. Kobayashi, M.M. Elkind, Sublethal and potentially lethal damage repair on thermal neutron capture therapy, Pigment Cell Res. 2 (1989) 337–342.

[2] A.D. Santin, P.L. Hermonat, A. Ravaggi, M. Chiriva-Internati, S. Pecorelli, G.P. Parham, Radiation-enhanced expression of E6/E7 transforming oncogenes of human papillomavirus-16 in human cervical carcinoma, Cancer 83 (1998) 2346–2352.

[3] G.L. Locher, Biological effects and therapeutic possibilities of neutrons, Am. J. Roentgenol. Radiat. Ther. 36 (1936) 1–13.

[4] J.A. Coderre, G.M. Morris, The radiation biology of boron neutron capture therapy, Radiat. Res. 151 (1999) 1–18.

[5] D.N. Slatkin, A history of boron neutron capture therapy of brain tumors—postulation of a brain radiation dose tolerance limit, Brain 114 (1991) 1609–1610.

[6] J.A. Coderre, Radiation oncology, in: S.A. Leibel, T.L. Phillips (Eds.), Textbook of Radiation Oncology, W. B. Saunders, Philadelphia, 1998, pp. 1263–1277.

[7] H. Hatanaka, Boron-neutron capture therapy for tumors, in: A.B.M.F. Karim, E.R. Laws (Eds.), Glioma, Springer, Berlin, 1991, pp. 233–249.

[8] M.A. Davis, J.B. Little, Relative biological effectiveness of the ^{10}B(n/alpha)^{7}Li reaction in HeLa cells, Radiat. Res. 43 (1970) 534–553.

[9] M. Javia, G.L. Brownell, W.H. Sweet, The possible use of neutron-capturing isotopes such as boron10 in the treatment of neoplasms. II. Computation of the radiation energies and estimates of effects in normal and neoplastic brain, J. Clin. Invest. 31 (1952) 604–610.

[10] E.I. Tolpin, G.R. Wellum, F.C. Dohan, Jr., P.L. Kornblith, R.G. Zamenhof, Boron neutron capture therapy of cerebral gliomas. II. Utilization of the blood-brain barrier and tumor-specific antigens for the selective concentration of boron in gliomas, Oncology 32 (1974) 223–246.

[11] D.E. Wazer, R.G. Zamenhof, O.K. Harling, et al., Boron neutron capture therapy, in: P.M. March, J.S. Loeffler (Eds.), Radiation Oncology Technology and Biology, W. B. Saunders, Philadelphia, 1994, pp. 167–191.

[12] K. Ono, Y. Kinashi, S. Masunaga, M. Suzuki, M. Takagaki, Electroporation increases the effect of borocaptate (10B-BSH) in neutron capture therapy, Int. J. Radiat. Oncol. Biol. Phys. 42 (1998) 823–826.

[13] C. Bauer, D. Gabel, U. Dörfler, Azanonaboranes [(RNH2B8H11NHR] as possible new compounds for use in boron neutron capture therapy, Eur. J. Med. Chem. 37 (2002) 649–657.

[14] K. Braun, P. Peschke, R. Pipkorn, S. Lampel, M. Wachsmuth, W. Waldeck, E. Friedrich, J. Debus, A biological transporter for the delivery of peptides to the nuclear compartment in living cells, J. Mol. Biol. 318 (2002) 237–243.

[15] A. Paquet, Introduction of 9-fluorenylmethyloxycarbonyl, trichloroethoxycarbonyl, and benzyloxycarbonyl amine protecting groups into O-unprotected hydroxyamino acids using succinimidyl carbonates, Can. J. Chem. 60 (1982) 976–980.

[16] C.G. Fields, D.H. Lloyd, R.L. MacDonald, K.H. Ottesan, R.L. Noble, HBTU activation for automated Fmoc-solid-phase peptide synthesis, Pept. Res. 4 (1991) 95–101.

[17] G. Wolber, K.H. Hoever, O. Krauss, W. Maier-Borst, A new fast-neutron source for radiobiological research, Phys. Med. Biol. 42 (1997) 725–733.

[18] K.H. Beckurts, K. Wirtz, Neutron Physics, Springer Verlag, Berlin, Göttingen, Heidelberg, New York, 1964. Library of Congress Catalog Card Number 64-25646.

[19] K.H. Hoever, Masters Thesis (Diplomarbeit), University of Heidelberg and DKFZ, 1971.

[20] A.H.W. Nias, D. Greene, M. Fox, et al., Effect of 14 MeV monoenergetic neutrons on HeLa and P388F cells in vitro, Int. J. Radiat. Biol. Relat. Stud. Phys. Chem. Med. 13 (1967) 449.

[21] G. Wolber, K. Braun, A. Eisenmenger, T. Sobkowiak, A. Bankamp, W. Semmler, Untersuchungen zur Bor-Neutronen-Einfang-Therapie (BNCT) in Feldern schneller Neutronen, in: K. Welker, K. Zink, (Eds.), Medizinische Physik., Berlin, 2001, pp. 273–274.

[22] V. Ehemann, B. Hashemi, A. Lange, H.F. Otto, Flow cytometric DNA analysis and chromosomal aberrations in malignant glioblastomas, Cancer Lett. 138 (1999) 101–106.

[23] L. Hampson, E.S. El Hady, J.V. Moore, H. Kitchener, I.N. Hampson, The HPV16 E6 and E7 proteins and the radiation resistance of cervical carcinoma, FASEB J. 15 (2001) 1445–1447.

[24] M.R. Loken, Immunofluorescence techniques, in: M.R. Melamed, T. Lindmo, M.L. Mendelsohn (Eds.), Flow Cytometry and Cell Sorting, 2nd ed. (Chapter 17), Wiley-Liss Inc, New York, 1990, pp. 341–353.

[25] E.L. Kreimann, M.E. Itoiz, A. Dagrosa, R. Garavaglia, S. Farias, D. Batistoni, A.E. Schwint, The hamster pouch as a model of oral cancer for boron neutron capture therapy studies: selective delivery of boron by boronophenylalanine, Cancer Res. 61 (2001) 8775–8781.

[26] S. Heckl, J. Debus, J. Jenne, R. Pipkorn, W. Waldeck, H. Spring, R. Rastert, C.W. von der Lieth, K. Braun, CNN-Gd(3+) enables cell nucleus molecular imaging of prostate cancer cells: the last 600 nm, Cancer Res. 62 (2002) 7018–7024.